RSC Advances

ROYAL SOCIETY OF CHEMISTRY

www.rsc.org/advances

Photodegradation of Rhodamine B in α-FeOOH/oxalate under light irradiation

Rufen Chen*[a,b], Xiaonian Zhang[a], Hui Liu[a], Xiuqin Song[a], Yu Wei*[,a]

(a. College of Chemistry and Material Science, Hebei Normal University, Shijiazhuang, 050024, P.R.China)

(b. Key Laboratory of Inorganic Nanomaterial of Hebei Province, Shijiazhuang 050024, China)

Abstract: High- and low-crystalline goethite (α-FeOOH) were obtained via air oxidation of $Fe(OH)_2$. Rhodamine B (RhB) was selected as a model pollutant, and the photocatalytic activity of the α-FeOOH/oxalate system under light irradiation was evaluated. The crystal structure, morphology, and specific surface area of the prepared α-FeOOH samples were determined by X-ray diffraction (XRD), transmission electron microscopy (TEM), and Brunauer–Emmett–Teller (BET), respectively. The adsorption behavior of α-FeOOH was determined using the Langmuir model. The effects of initial pH value, initial concentration of oxalic acid, and light intensity on RhB photodegradation were investigated in the α-FeOOH/oxalate suspension. In contrast to high-crystalline α-FeOOH, low-crystalline α-FeOOH with high specific surface shows higher adsorption and photocatalytic activity toward RhB photodegradation by a photo-Fenton-like reaction. A possible mechanism for RhB degradation was also suggested.

---

* Corresponding author. Tel.: 86031170787400.

E-mail: chenrufen@139.com(R. Chen), weiyu@mail.hebtu.edu.cn(Y. Wei).

Keywords: α-FeOOH; Oxalic acid; Light irradiation; Rhodamine B; Photodegradation

1. Introduction

Dye pollutants produced from industries are becoming a major source of environmental contamination [1]. Rhodamine B (RhB) is an important dye that is widely used in the textile industry. Thus, its removal from wastewater is of great importance [2-3]. The Fenton reaction is known to be a highly effective method for removing dye pollutants for wastewater treatment [1, 4-5]. Highly reactive hydroxyl radicals (•OH) can form during the Fenton reaction and degrade organic compounds [6–7]. In the traditional Fenton system, H_2O_2 is a direct source of •OH [8-9]. When light and organic acids are introduced to the treatment system, H_2O_2 can be self-produced without further addition of H_2O_2. Then, •OH can be generated by a photo-Fenton-like reaction [10-11].

In fact, numerous natural transformation processes in the aquatic environment can also clear away organic pollutants. Iron oxides (including oxyhydroxides) and oxalic acid, which coexist in natural aquatic environments, can set up a photo-Fenton-like system under light irradiation to degrade organic pollutants [12–14]. Iron oxides are extensively found in soils, lakes, and rivers [1]. Oxalic acid possesses strong chelating ability with multivalent cations and is mainly exuded by plant roots in the natural environment [15]. Light-irradiated heterogeneous Fe(III)/oxalate systems can also achieve high efficiencies in degrading organic contaminants [16].

Goethite (α-FeOOH) is the α-form of oxyhydroxide. α-FeOOH, which presents a large surface area and stable chemical properties, can be used as an adsorbent and catalyst in water

treatment [17-19]. Hence, the preparation of highly active α-FeOOH is important in modern environmental chemistry. Previous studies on pollutant photodegradation in the α-FeOOH system generally involve the use of highly crystalline α-FeOOH as photo-Fenton catalysts [20-21]. In our previous investigation, both light and the presence of trace amounts of ethylenediaminetetracetic acid（EDTA）increased reaction rates. Relatively high oxidation rates favor the formation of the highly active, low-crystalline α-FeOOH phase, which can transform into α-Fe_2O_3 [22-23]. However, the photocatalytic properties of low-crystalline α-FeOOH require further discussion.

Herein, we prepared high- and low-crystalline α-FeOOH by air oxidation of $Fe(OH)_2$ at room temperature. The photodegradation of RhB in the α-FeOOH/oxalate suspension under light irradiation was investigated in detail.

2. Experimental Section

2.1. Materials

Sodium hydroxide (NaOH), ethylenediaminetetracetic acid(EDTA), sulfuric acid (H_2SO_4), hydrochloric acid (HCl), 5,5-dimethyl-1-pyrroline-N-oxide (DMPO) and Rhodamine B (RhB) were purchased from Tianjin Chemical Reagents Company (the purities are 99%), and were used as received without further purification. Aqueous ferrous sulfate ($FeSO_4$) solution was prepared by dissolving iron granule in 20% H_2SO_4. Distilled water was used as solvent for the reactions.

2.2. Preparation of the high- and low-crystalline α-FeOOH samples

The α-FeOOH samples were prepared by air oxidation of $Fe(OH)_2$ under irradiation by

visible light in the presence of trace EDTA at pH 8.7. And the high-crystalline and low-crystalline α-FeOOH samples were obtained in the presence of EDTA (1mM) by controlling the light intensities at 0, and 150 lux, respectively, which was reported in our previous study [22].

2.3 Adsorption experiments

The adsorption experiments of RhB on the α-FeOOH surface were conducted at 20 °C in the dark. A fixed amount of α-FeOOH (0.1 g) was added to 100 mL of an aqueous RhB solution with various concentrations, which remained for 6 h in a vibrator unit in the dark under N_2 at 20 °C. RhB concentrations were measured after equilibrium by a spectrophotometer (SP-752, Shanghai) at a wavelength of 554 nm, using a 1 cm quartz cell, and the amount of RhB adsorbed on the α-FeOOH was calculated based on the mass balance according to Eq. (1) [24].

2.4 Measurement of photocatalytic activity

The photocatalytic degradation of RhB using high- and low-crystalline α-FeOOH was carried out as follows. A fixed amount of α-FeOOH (0.1 g) was added to 100 mL of RhB solution (0.01 mmol/L). The RhB and α-FeOOH were stirred for 60 min in the dark to ensure adsorption equilibrium. And then, light irradiation was performed by means of high-pressure Hg-lamp (wavelength range from 200 to 700, the main wavelength was 365 nm) with different light intensity. The light intensity (E) was detected by a light meter (TES-1336A). The solution pH was adjusted with diluted solutions of HCl and NaOH. At selected time intervals, 5 mL aliquots were collected, filtered, and analyzed by the spectrophotometer. All experimental runs were performed at 20 ◦C under continuous stirring in the presence of light

and air. The H_2O_2 concentrations in the filtrates were determined using a H_2O_2 – photometer at LED 528 nm. The concentrations of Fe(III) and Fe(II) in solution were determined by the 1,10-phenanthroline method [25].

2.5 Sample characterizations

X－ray diffraction (XRD) patterns were obtained on a Bruker diffractometer using a Cu Kα radiation. The crystallinity of samples were determined from the peak area between 2 θ = 21.2 and 36.7° using a highly crystalline α-FeOOH sample (supplied by Tianjin Chemical Reagents Company) as a reference. X-ray photoelectron spectroscopy (XPS) was performed in an ion pumped VG Microtech CLAM4 MCD analyser systemusing 200 W unmonochromated Mg X-ray excitation. Transmission electron microscopy (TEM) images were obtained by a Hitachi H-7500 transmission electron microscope. The specific surface area of the iron oxides was determined by multipoint N_2-BET analysis using a Quantachrome (NOVAe) surface area analyzer. Electron spin resonance (ESR) spectra were obtained using a Bruker model ESP 300E electron paramagnetic resonance spectrometer equipped with a quanta-Ray Nd:YAG laser system as the irradiation light source (λ = 355 nm). The settings were center field, 3480.00 G; microwave frequency, 9.79 GHz; power, 5.05mW. Total organic carbon (TOC) analysis was carried out by means of a Shimadzu TOC-V CPH total organic carbon analyzer.

3. Results and Discussion

3.1 Preparation and properties of α-FeOOH samples

Figure 1(A) shows the XRD patterns of the iron oxide prepared by air oxidation of

$Fe(OH)_2$ in the presence of EDTA (1mM) with and without light irradiation (light intensities: a: 0lux; b: 150lux). All diffraction peaks could be definitely assigned to the α-FeOOH phase (JCPDS: 29-0713); this result indicates that the samples are phase-pure α-FeOOH. The crystallinities of obtained α-FeOOH in the presence of trace EDTA with and without visible light irradiation were 48.9 % and 7.1 %, respectively. Furthermore, the Fe 2p region in the XPS spectrum of obtained product in the presence of trace EDTA with visible light irradiation, was also used to investigate the valence states of Fe ion (Fig.1(B)). The typical peaks of Fe element at the binding energies of 724.6eV (Fe2p1/2) and 711.0eV (Fe2p3/2) are found. The energy separation between Fe2p1/2 and Fe2p3/2 is 13.6eV, which is a characteristic of FeOOH [26]. And a satellite peak of Fe2p3/2 can be seen in about 719.0 eV, as shown in Fig.1(B). The results also indicate that only Fe^{3+} is present in product [27], which is also in accord with the result of XRD spectrum.

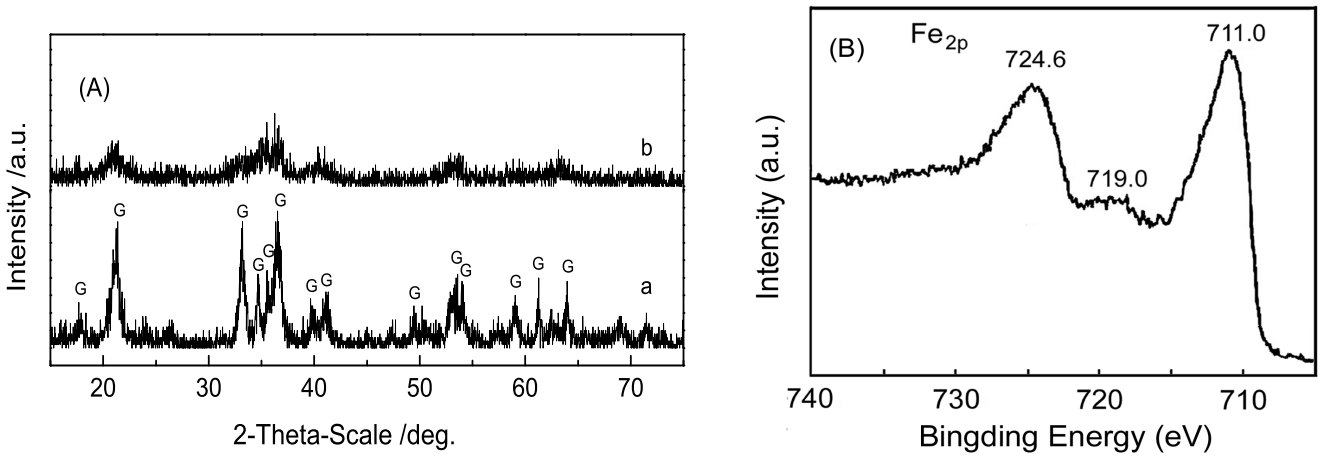

Fig.1(A) XRD patterns of samples in the presence of EDTA with and without light irradiation (light intensities: a: 0 lux; b: 150 lux; G: α-FeOOH); (B) Fe 2p region in the XPS spectrum of the sample in the presence of EDTA with light irradiation

TEM images of obtained α-FeOOH samples are shown in Fig.2. Correlating the results shown in Figs. 1 and 2, we can see that the relatively low-crystalline α-FeOOH (L-α-FeOOH) and high-crystalline α-FeOOH (H-α-FeOOH) samples are obtained in the presence of trace EDTA with and without visible light irradiation. The specific surface area (SSA) and total pore volume (TPV) of L-α-FeOOH and H-α-FeOOH are listed in Table 1. L-α-FeOOH clearly possesses a higher specific surface area and total pore volume than H-α-FeOOH.

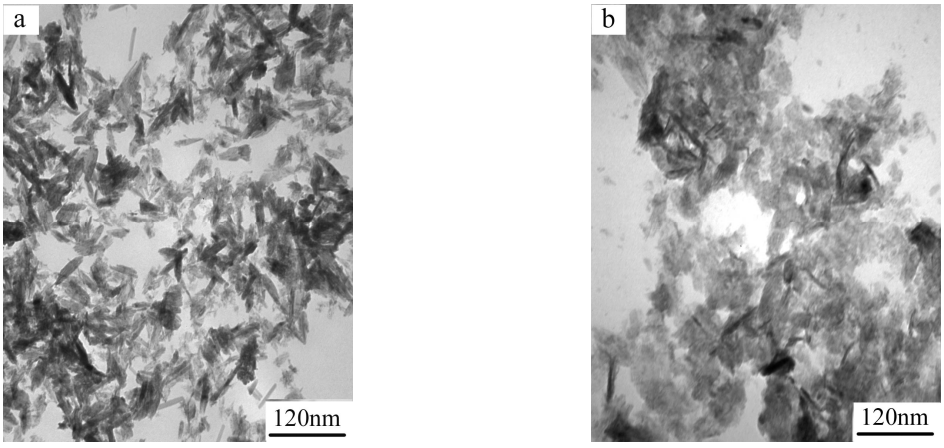

Fig.2 TEM images of samples in the presence of EDTA with and without light irradiation (light intensities: a: 0 lux; b: 150 lux)

The difference in reaction rates may be the main reason for the variations observed. The concentration of Fe (Ⅱ) (solid and liquid) was monitored during the oxidation (15 mL of the suspension was taken out at different time and dissolved in 20% H_2SO_4, determined by the 1,10-phenanthroline method [25]). As shown in Fig. 3, the concentration of Fe(II) decreases rapidly in the reaction under visible light irradiation in the presence of trace EDTA (Fig.3c). The oxidation speed of reaction under visible light irradiation in the presence of trace EDTA is obviously more rapid than that at short of light irradiation or EDTA systems. During the

oxidation of Fe(II), EDTA is chelated with Fe(II), forming FeII-EDTA complexes, which can absorb light in the visible regions and produce oxidizing species [22-23], leading to the acceleration of the oxidation rate. The crystal seeds of α-FeOOH are formed too rapidly, and there are too many to grow in a short time. Consequently, low-crystalline α-FeOOH is obtained.

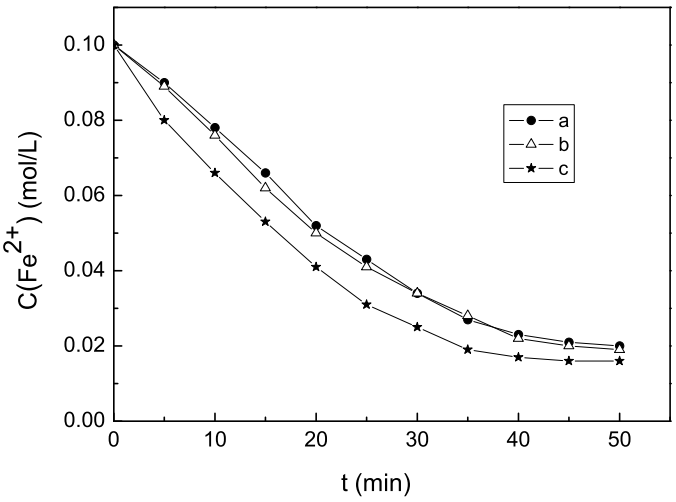

Fig.3 Changes of the Fe (Ⅱ) concentration with reaction time at different light intensities with and without EDTA (a: in the presence of EDTA and light intensities (0 lux); b: in the absence of EDTA and light intensities (150 lux); c: in the presence of EDTA and light intensities (150 lux))

3.2 Adsorption of RhB II by α-FeOOH samples

The adsorption isotherms of RhB on the prepared H-α-FeOOH and L-α-FeOOH samples are shown in Fig. 4. These isotherms exhibited best fit with the Langmuir adsorption model, as shown in Eq. (1) [24, 28].

$$\frac{C_e}{\Gamma} = \frac{1}{\Gamma_{max}} \mathbf{C_e} + \frac{1}{K_\alpha \Gamma_{max}} \quad (1)$$

C_e and Γ_{max} (mol/g) are the adsorbed concentration and saturated adsorption capacity, respectively, and K_a (L/mol) is the adsorption equilibrium constant. The Γ_{max} and K_a values of RhB on the prepared H-α-FeOOH and L-α-FeOOH samples are listed in Table 1. The Γ_{max} values can be ranked in the order of L-α-FeOOH > H-α-FeOOH, whereas the order of K_a can be ranked as L-α-FeOOH > H-α-FeOOH. In principle, a higher value of physical adsorption corresponds to a larger specific surface area and lower crystallization. Similarly, a larger K_a value denotes stronger chemical adsorption [29]. Given these considerations, the results obtained in this study imply that the L-α-FeOOH shows higher physical and chemical adsorption than that of the H-α-FeOOH.

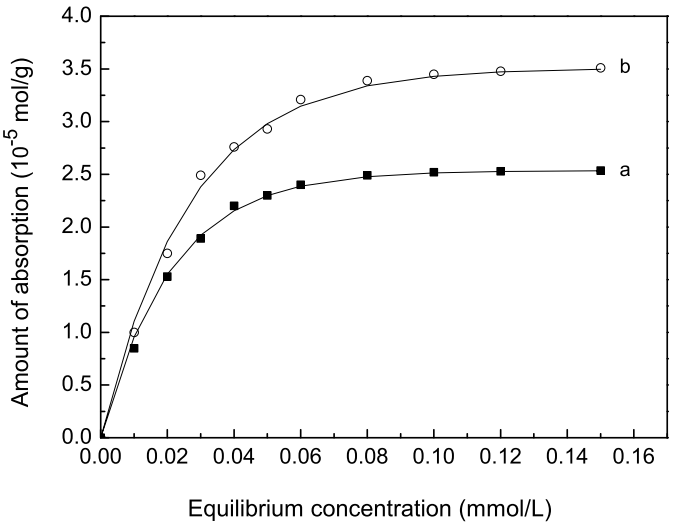

Fig.4 Adsorption isotherms of RhB on the H-α-FeOOH(a) and L-α-FeOOH(b)

Table1 Adsorption parameters of RhB by using the H-α-FeOOH and L-α-FeOOH

Samples	SSA (m^2/g)	TPV ($cm^3.g^{-1}$)	$\Gamma_{max} \times 10^{-5}$ (mol/g)	$K_a \times 10^4$ (L/mol)	R^2
H-α-FeOOH	139.5	0.17	2.530	2.52	0.9972
L-α-FeOOH	211.7	0.22	3.507	2.87	0.9960

3.3 Photocatalytic oxidation of RhB

3.3.1 Effect of initial pH

Experiments were carried out at different pH values to select an optimum pH for RhB degradation. In this investigation, the effect of initial pH value on RhB degradation in the α-FeOOH/oxalate system was studied at initial pH ranging from 2 to 8. Fig. 5 shows the dependence of RhB degradation on initial pH in the L-α-FeOOH/oxalate system in the presence of L-α-FeOOH and oxalate (1.0 mM) under light irradiation (1000.0 lux). The optimal initial pH is approximately 3.0. The α-FeOOH/oxalate system at an initial pH of 3.0 may present a higher concentration of $[\equiv FeIII(C_2O_4)_n]^{3-2n}$, which allows generation of more •OH [30]. As the pH increases further (pH > 3), $[\equiv FeIII(C_2O_4)_n]^{3-2n}$ concentrations could decrease and induce low photoactivity. At a lower initial pH of 2, complexation of L-α-FeOOH and oxalate is hindered, leading to lower RhB degradation [24]. According to data in Fig. 5, pH = 3 was selected for subsequent experiments.

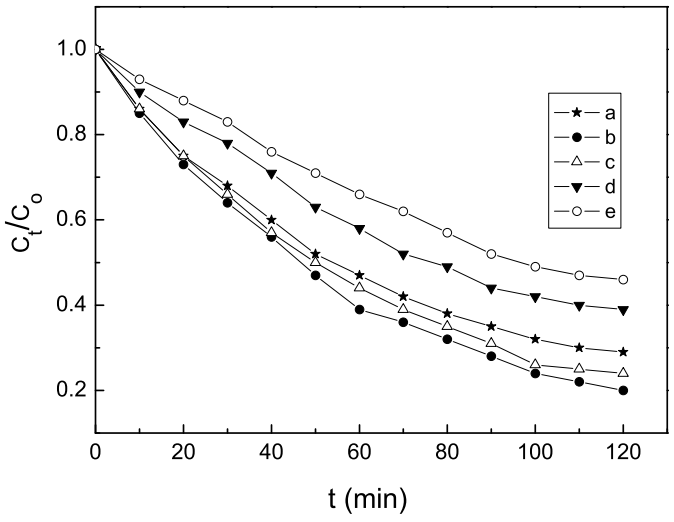

Fig.5 Effect of initial pH on the RhB degradation in the L-α-FeOOH/oxalate system under light irradiation (a: pH = 2; b: pH = 3; c: pH = 4; d: pH = 6; e: pH = 8)

3.3.2 Effect of initial concentration of oxalic acid

Fig.6 shows the dependence of RhB photodegradation on the initial concentration of oxalic acid (C_0) under light irradiation (1000.0 lux) at pH 3. The photodegradation rate of RhB increases with increasing concentration of oxalic acid from 0.0 mM to 1.0 mM. In the absence of oxalate, iron oxides act as photocatalysts and can be excited to generate electron–hole pairs despite the lower rate of RhB degradation [31]. In the presence of oxalate, iron oxide–oxalate complex forms, and a photo-Fenton-like system is set up. The presence of iron oxide and oxalate in cooperation has been confirmed to substantially accelerate the degradation of RhB. However, RhB degradation decreases at oxalic acid concentrations exceeding 1.0 mM. Excessive oxalate can occupy adsorption sites on the surface of α-FeOOH, possibly hindering RhB adsorption on the α-FeOOH surface. Thus, not all of the OH• radicals are utilized by RhB [24], which leads to decreases in RhB degradation. These results indicate that the concentration of oxalic acid is a vital factor influencing the α-FeOOH/oxalate system for RhB degradation. The optimal concentration of oxalic acid in the α-FeOOH/oxalate system is determined to be 1.0 mM.

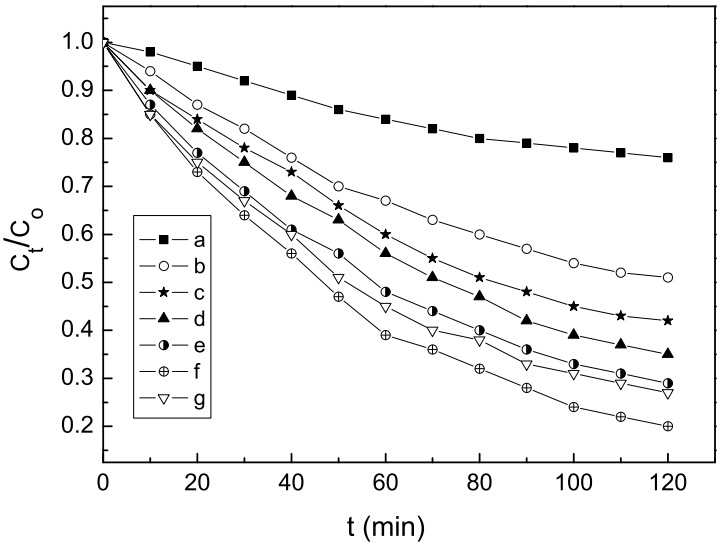

Fig.6 Effect of initial concentration of oxalic acid (C_0) on the RhB degradation in the L-α-FeOOH/ oxalate system under light irradiation (a: C_0 = 0.0 mM; b: C_0 = 0.2 mM; c: C_0 = 0.4 mM; d: C_0 = 0.6 mM; e: C_0 = 0.8 mM; f: C_0 = 1.0 mM; g: C_0 = 1.2 mM)

3.3.3 Effect of light intensity

Experiments were carried out to investigate the effect of light intensity (E) on RhB degradation in the L-α-FeOOH/oxalate system using the optimal pH and oxalic acid concentration. Fig. 7 shows the dependence of RhB photodegradation on light intensity (E) in the L-α-FeOOH/oxalate system. In this investigation, higher light intensities can lead to higher degradation rates of RhB during photochemical reaction. However, further increases in light intensity beyond 1000.0 lux do not result in significant increases in RhB photodegradation.

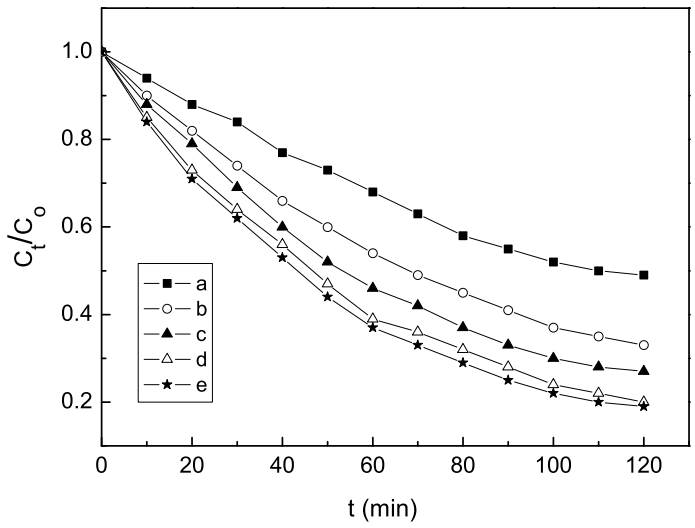

Fig.7 Effect of light intensity on the RhB degradation in the L-α-FeOOH/oxalate system (a: E= 0.0 lux; b: E= 200.0 lux; c: E= 500.0 lux; d: E= 1000.0 lux, e: E=1500.0lux)

The foregoing results indicate that L-α-FeOOH, oxalate, and light at pH 3 provide the most effective conditions for RhB degradation in the L-α-FeOOH/oxalate system. In our

study, the effects of initial pH value, initial oxalic acid concentration, and light intensity on RhB photodegradation in the H-α-FeOOH system present the same change trend as that in L-α-FeOOH.

3.3.4 Photodegradation of RhB in the α-FeOOH/oxalate suspension

Fig. 8 shows the photodegradation of RhB at pH 3 under light irradiation (1000.0 lux) at different conditions. Without oxalic acid and with only H-α-FeOOH (Fig. 8a) and L-α-FeOOH (Fig. 8b), lower degradation of RhB may be seen. In particular, with only H-α-FeOOH as a photocatalyst, RhB degradation is almost negligible. However, when systems with 1.0 mM oxalic acid are subjected to the same conditions as in curves a and b, RhB degradation rates evidently increase under light irradiation. L-α-FeOOH shows higher catalytic activity toward RhB photodegradation than H-α-FeOOH. The TOC removal efficiencies of RhB in the H-α-FeOOH and L-α-FeOOH systems in the presence of 1.0 mM oxalic acid at pH 3 under light irradiation (1000.0 lux) are shown in Fig. 9. The TOC removal efficiencies of RhB in the H-α-FeOOH/oxalate and L-α-FeOOH/oxalate systems after 120 min are 47.8% and 62.6%, respectively. The results indicate that RhB can effectively undergo degradation and mineralization during the reaction.

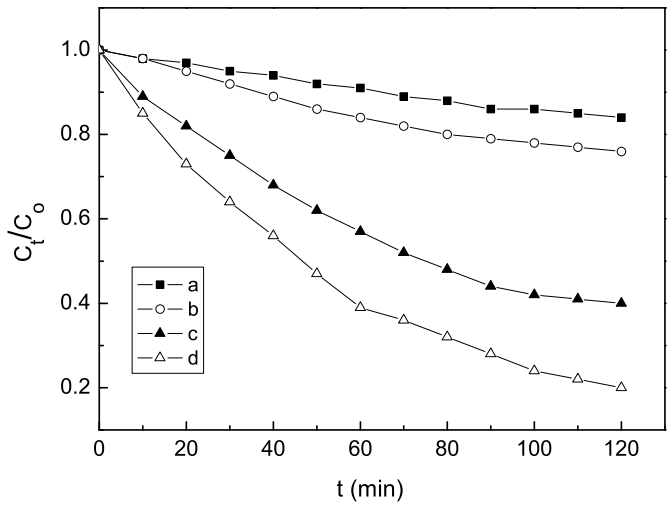

Fig.8 Photodegradation of RhB under light irradiation at different conditions (a: H-α-FeOOH; b: L-α-FeOOH ; c: H-α-FeOOH/oxalate; d: L-α-FeOOH/oxalate)

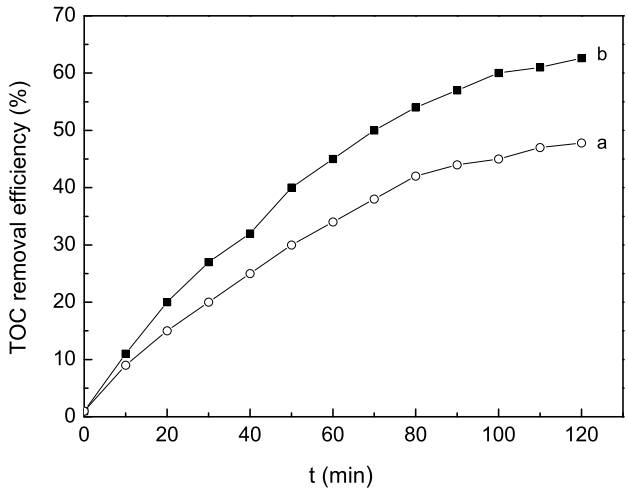

Fig.9 TOC removal efficiency of RhB versus the reaction time in the H-α-FeOOH/oxalate(a) and L-α-FeOOH/oxalate(b) systems

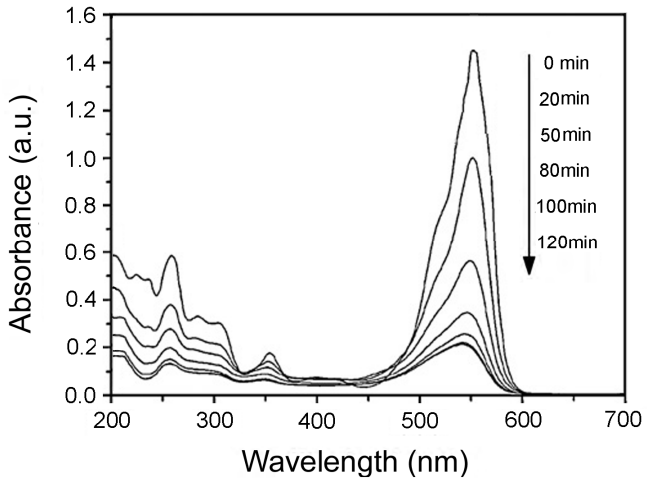

Fig.10 UV-vis spectral changes of RhB in the L-α-FeOOH/oxalate system

Fig. 10 shows UV–visible spectral changes during RhB degradation in L-α-FeOOH with 1.0 mM oxalic acid at pH 3 under light irradiation (1000.0 lux). RhB exhibits a main

absorption peak at 554 nm and two minor absorption peaks at 255 and 355 nm. The same absorption spectra of RhB were observed by Yang Y. et al [32]. As irradiation time increases, the RhB absorption peak decreases to different extents without peak shifting, which suggests that degradation proceeds through oxidation instead of de-ethylation of the RhB molecule [33].

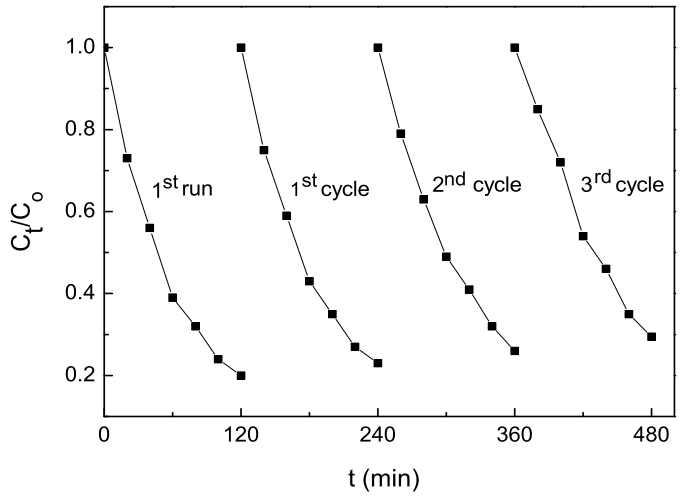

Fig. 11 Stability of L-α-FeOOH catalyst after subsequent reactions under identical conditions (1.0 mM oxalic acid, pH 3, light irradiation (1000.0 lux))

To evaluate the stability of prepared catalysts, catalytic performance of α-FeOOH with 1.0 mM oxalic acid at pH 3 under light irradiation (1000.0 lux) was tested in three subsequent oxidation cycles under identical conditions. After each experiment, the catalyst was separated from treated solution by centrifugal separator, washed with distilled water, dried and used for next run. Obtained results indicate that the L-α-FeOOH photocatalyst can be reused effectively for several times without significant losses in activity (Fig.11). After recycling L-α-FeOOH for three times, the RhB degradation rate ranges from 80.0 % to 70.5 %. This

finding suggests that the photocatalytic activity of prepared L-α-FeOOH catalyst is not easily lost even after recycling. Meanwhile, we find that the stability of H-α-FeOOH is a little higher than that of L-α-FeOOH.

3.3.5 Possible photocatalytic mechanism

During photoreaction, oxalic acid is initially adsorbed by iron oxide particles to form $[Fe(C_2O_4)_n]^{3-2n}$ (Eq.2). H_2O_2 can be self-produced under light irradiation (Eqs.3-7). Changes in H_2O_2 concentration with reaction time at different conditions under light irradiation (1000.0 lux) are shown in Fig. 12. Figs. 12(A) and 12(B) show that the concentrations of H_2O_2 increase with reaction time, particularly at earlier stages of reaction [34]. As the reaction progresses, the concentration of H_2O_2 tends to decrease gradually. This trend can be explained by the fact that the H_2O_2 in the system reacts with Fe^{2+}, which leads to observable decreases in H_2O_2 concentration at later stages of reaction. As shown in Fig. 12(A), the concentration of H_2O_2 increases faster in the reaction system with oxalic acid than in the reaction system without oxalic acid. The concentration of H_2O_2 formed in the L-α-FeOOH/oxalate system [Fig. 12(A)d] is higher than that formed in the H-α-FeOOH/oxalate system [Fig. 12(A)c]. Fig. 12(B) shows that the concentration of H_2O_2 increases with increasing oxalic acid concentration from 0.0 mM to 1.0 mM. It has been confirmed that iron (hydr) oxides can catalyze the decomposition of H_2O_2 and form OH• radicals [35]. In our case, excess oxalate (C_0 = 1.2 mM) can occupy adsorption sites on the surface of α-FeOOH and inhibit H_2O_2 formation, which can lead to decreased RhB degradation (Fig. 6g).

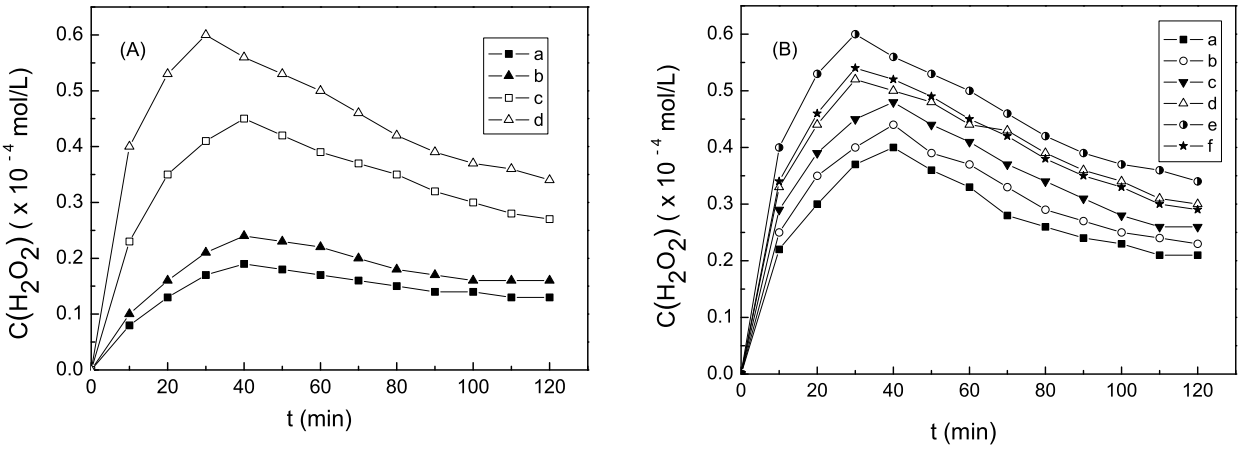

Fig.12 Changes of the H_2O_2 concentration with reaction time: (A): (a: H-α-FeOOH; b: L-α-FeOOH; c: H-α-FeOOH in the presence of 1.0mM oxalic acid; d: L-α-FeOOH in the presence of 1.0 mM oxalic acid); (B): L-α-FeOOH system in the presence of different concentrations of oxalic acid (C_0) (a: C_0 = 0.2 mM; b: C_0 = 0.4 mM; c: C_0 = 0.6 mM; d: C_0 = 0.8 mM; e: C_0 = 1.0 mM; f: C_0 = 1.2 mM)

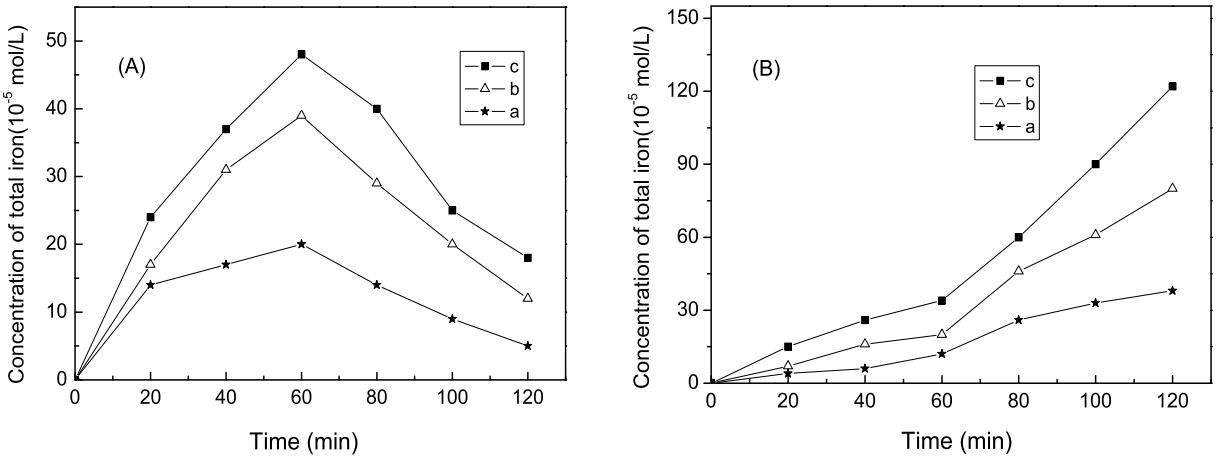

Fig.13 The concentration of the dissolved Fe(III) (A) and Fe(II) (B) vs. reaction time by using different samples: (a: L-α-FeOOH; b: H-α-FeOOH/oxalate; c: L-α-FeOOH/oxalate)

Iron oxides could be photodissolved during the photoreaction. The dissolved Fe(III) species could be photoreduced to generate Fe(II) species [1]. Fig. 13(A) shows that the concentrations of Fe(III) increase with the reaction time in the earlier stages of the reaction (0–60 min). As the reaction progresses, the concentration of Fe(III) tends to decrease gradually. And the concentrations of Fe(II) increase with the reaction time (Fig.13(B)). During the reaction under light irradiation, the Fe(III) species are readily reduced to form Fe(II), thereby leading to the observed decrease in the concentration of Fe(III) in the later stages of the reaction, and increase in the concentration of Fe(II). Meanwhile, from Fig. 13(A) and (B) we can see that the concentrations of dissolved Fe(III) and Fe(II) in the system are higher in the presence of oxalic acid (C_0 = 1.0 mM) than without oxalic acid, which indicate that oxalic acid can promote α-FeOOH dissolution. And the concentrations of dissolved Fe(III) and Fe(II) in the L-α-FeOOH/oxalate system are higher than that in the H-α-FeOOH/oxalate system, which indicate that L-α-FeOOH is easily dissolved. Formation of Fe(III) and Fe(II) species in aqueous solution during reaction performs a critical function in RhB degradation. The system obtains higher concentration of Fe(II) ions, and will exhibit higher RhB degradation efficiency based on homogeneous Fenton reaction (Eqs. 6-8).

Increased RhB adsorption on L-α-FeOOH is expected to enhance RhB photodegradation in the L-α-FeOOH/oxalate system [28]. Upon light irradiation, electron–hole pairs are photogenerated on the surface of the α-FeOOH catalyst. Fe(III) on the surface of α-FeOOH (≡Fe(III)) can combine with H_2O_2 to form OH• by heterogeneous Fenton reaction, as shown in Eqs. (9–10). Then, the OH• formed in the system reacts with dye molecules to form other species; thus, OH• is responsible for dye degradation.

Surface-adsorbed organic compounds are readily oxidized by OH• radicals. Consequently, besides showing higher adsorption for RhB II, L-α-FeOOH also exhibits higher photocatalytic degradation activity.

Furthermore, ESR tests with DMPO were conducted to detect •OH radicals produced in the L-α-FeOOH system in the presence of 1.0mM oxalic acids at pH 3 under light irradiation (1000.0lux). As shown in ESR spectra (Fig. 14), the intensity ratio of main peaks belonged to DMPO-•OH in the L-α-FeOOH/ oxalate system is 1:2:2:1under 355 nm laser irradiation. And the intensities of signal strengthen with increased irradiation time, indicating the concentrations of •OH radicals increase with the irradiation time prolonged. This indicates that the •OH radicals is surely formed in the system [36-37]. •OH radicals can be mainly responsible for the RhB degradation (Eq. 11).

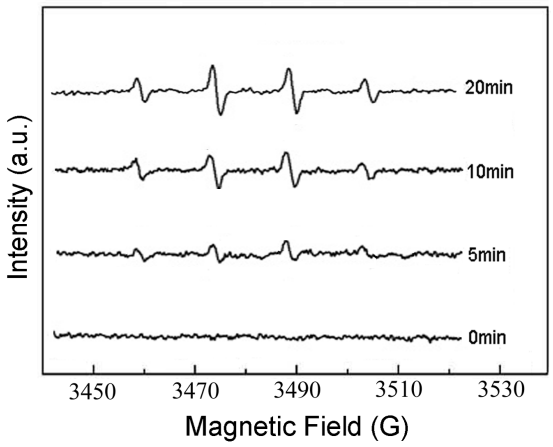

Fig.14 DMPO spin-trapping ESR spectra in the L-α-FeOOH/oxalate aqueous dispersion

The possible reactions for the RhB degradation are given as follows:

$$\text{Iron oxide} + n H_2C_2O_4 \rightarrow [\ Fe(C_2O_4)_n]^{3-2n} \quad (2)$$

$$[Fe^{III}(C_2O_4)n]^{3-2n} + h\nu \rightarrow [Fe^{II}(C_2O_4)_{(n-1)}]^{4-2n} + (C_2O_4)\bullet^{-} \quad (3)$$

$(C_2O_4)\bullet^- \rightarrow CO_2 + CO_2\bullet^-$ (4)

$CO_2\bullet^- + O_2 \rightarrow CO_2 + O_2\bullet^-$ (5)

$O_2\bullet^- + Fe^{3+} \rightarrow Fe^{2+} + O_2$ (6)

$O_2\bullet^- + nH^+ + Fe^{2+} + h\nu \rightarrow Fe^{3+} + H_2O_2$ (7)

$Fe^{2+} + H_2O_2 \rightarrow Fe^{3+} + OH^- + \bullet OH$ (8)

$\equiv Fe(III) + H_2O_2 \rightarrow \equiv Fe(II) + HO_2\bullet + H^+$ (9)

$\equiv Fe(II) + H_2O_2 \rightarrow \equiv Fe(III) + OH\bullet + OH^-$ (10)

$RhB + OH\bullet \rightarrow$ Products (11)

4. Conclusions

High- and low-crystalline α-FeOOH were obtained via air oxidation of $Fe(OH)_2$. The oxalic acid concentration, initial pH, and light intensity were vital factors influencing the α-FeOOH/oxalate system for RhB degradation. Under light irradiation and optimal pH of 3, the optimal oxalic acid concentration in the α-FeOOH/oxalate system for RhB degradation was determined to be 1.0 mM. Higher light intensity also led to higher RhB degradation rates. In contrast to high-crystalline α-FeOOH, low-crystalline α-FeOOH possessed a larger specific surface area, was more easily dissolved in aqueous solution, and could produce higher H_2O_2 concentrations in the system; thus, α-FeOOH showed higher adsorption and photocatalytic activity toward RhB photodegradation by homogeneous and heterogeneous photo-Fenton-like reactions. RhB degradation could be mainly attributed to the present of •OH radicals in the system.

Acknowledgment

This work was supported by the National Natural Science Foundation of China (21477032, 21277040), by the Natural Science Foundation of Hebei Province (B2013205069, B2012205041, B2014205085).

References

[1] J. Lei, C. Liu, F. Li, X. Li, S. Zhou, T. Liu, M. Gua, Q. Wu, J. Hazard Mater. B137 (2006) 1016–1024.

[2] C. Bai, W. Gong , D.Feng , M. Xian, Q. Zhou, S. Chen, Z. Ge, Y. Zhou, Chem. Eng. J. 197 (2012) 306–313.

[3] M.-F. Hou, L. Liao, W.-D. Zhang, X.-Y. Tang, H.-F. Wan, G.-C.Yin, Chemosphere. 83 (2011) 1279-1283

[4] E. Kusvuran, S. Irmak, H.I. Yavuz, A. Samil, O. Erbatur, J. Hazard. Mater. 119 (2005) 109–116.

[5] D.L. Sedlak, A.W. Andren, Environ. Sci. Technol. 25 (1991) 1419–1427.

[6] M. Pera-Titus, V. Garcia-Molina, M.A. Ba˜nos, J. Gim´enez, S. Esplugas, Appl. Catal. B 47 (2004) 219–256.

[7] M.L. Kremer, Phys. Chem. Chem. Phys. 1 (1999) 3595–3605.

[8] G.V. Buxton, C.L. Greenstock, W.P. Helman, A.B. Ross, J. Phys. Chem. Ref. Data 17 (1988) 513–886.

[9] W.R. Haag, C.C.D. Yao, Environ. Sci. Technol. 26 (1992)1005–1013.

[10] J. Kiwi, N. Denisov, Y. Gak, N. Ovanesyan, P.A. Buffat, E. Suvorova, F. Gostev, A. Titov, O. Sarkisov, P. Albers, V. Nadtochenko, Langmuir 18 (2002) 9054–9066.

[11] X. Tao, J. Su, J. Chen, J. Zhao, Chem. Commun. 36 (2005) 4607–4609.

[12] C. Siffert, B. Sulzberger, Langmuir 7 (1991) 1627–1634.

[13] B.C. Faust, J. Allen, Environ.Sci. Technol. 27 (1993) 2517–2522.

[14] Y.G. Zuo, Y.W. Deng, Chemosphere 35 (1997) 2051–2058.

[15] T. Kayashima, T. Katayama, Biochim. Biophys. Acta: Gen. Subj. 1573 (2002) 1–3.

[16] T. Zhou, X. Wu, Y. Zhang, J. Li, T-T. Lim, Applied Catalysis B: Environmental 136– 137 (2013) 294– 301

[17] H. Fukouka, N. SHigemoto, H. Inomo, W. Shiraki, J. Chem. Eng. Jpn. 41 (2008) 69–75.

[18] S. Simonetti, D. Damiani, A. Juan, G. Brizuela, Surf. Rev. Lett. 14 (2007) 209–217.

[19] Y. Li, F.S. Zhang, Chem. Eng. J. 158 (2010) 148–153.

[20] J. He, W. Ma, J. He, J. Zhao, J.C. Yu, Appl. Catal. B: Environ. 39 (2002) 211-220.

[21] J.J. Wu, M. Muruganandham, J.S. Yang, S.S. Lin, Catal. Commun. 7 (2006) 901-906.

[22] R. Chen, H. Chen, Y. Wei, J. Phys. Chem. C 111 (2007)16453-16459.

[23] R. Chen, G. Song, Y. Wei, J. Phys. Chem. C 114(2010)13409-13413.

[24] X. Wang, C. Liu, X. Li, F. Li, S. Zhou, J. Hazard. Mater. 153 (2008) 426-433.

[25] C. Paipa, M. Mateo, I. Godoy, E. Poblete, M.I. Toral, T. Vargas, Miner. Eng. 18 (2005) 1116-1119.

[26] Q. Huang, W. Wei, Q.Yan, C.Wu, X. Zhu, Mater. Lett. 152(2015)203 - 206

[27] L. Zeng, W. Ren, J. Zheng, A. Wua, P.Cui, Appl. Surf. Sci. 258 (2012) 2570 - 2575

[28] Y. Lin, Y.u Wei, Y. Sun, J. Mol. Catal. A: Chem. 353– 354 (2012) 67- 73.

[29] Y. Wang, Y. Zhao, Y. Ma, H. Liu, Y. Wei, J. Mole. Catal. A 325 (2010) 79- 83

[30] E. Balmer, B. Sulzberger, Environ. Sci. Technol. 33 (1999) 2418 - 2424.

[31] J. K. Leland, A.J. Bard, J. Phys. Chem. 91 (1987) 5076 - 5083.

[32] D. Li, H. Zheng, Q. Wang, X. Wang, W. Jiang, Z. Zhang, Y. Yang, Sep. Purif. Technol. 123 (2014) 130–138.

[33] J. Huang, D. Wang, L. Yin, L. Cao, H. Ouyang, J. Li, W. Hao, J. Alloys Compd. 612 (2014) 233–238.

[34] M. Pera-Titus, V. Garcia-Molina, M.A. Ba˜nos, J. Gim´enez, S. Esplugas, Appl. Catal. B 47 (2004) 219-256.

[35] Y. Ma, S. Meng, M.Qin, H. Liu, Y. Wei, J. Phys. Chem. Solids 73 (2012) 30–34.

[36] Y.Nie, C. Hu, J. Qu, X. Hu, J. Hazard. Mater. 154 (2008) 146–152.

[37] J. Yang, J. Dai, C. Chen, J. Zhao, J. Photoch. Photobio. A: Chem. 208 (2009) 66–77.